Defect and Diffusion Forum
ISSN: 1662-9507, Vol. 388, pp 135-145
doi:10.4028/www.scientific.net/DDF.388.135

Submitted: 2018-01-16
Revised: 2018-05-24
Accepted: 2018-05-30
Online: 2018-10-16

MHD Natural Convection Slip Flow through Vertical Porous Plates with Time-Periodic Boundary Conditions

Samuel O. Adesanya[1,3*], L. Rundora[2], R.S. Lebelo[3] and K.C. Moloi[3]

Department of Mathematical Sciences, Redeemer's University, Ede, Nigeria.

Department of Mathematics and Applied Mathematics, University of Limpopo, Turfloop Campus, Private Bag X1106, Sovenga 0727, South Africa.

Department of Education, Vaal University of Technology, Vanderbijlpark, 1911, South Africa

E-mail: *adesanyas@run.edu.ng

Keywords: Magnetic field; Buoyancy force; Ohmic heating; internal heat generation; Adomian Decomposition Method

Abstract. In this work, the convective flow of heat generating hydromagnetic fluid through a leaky channel is investigated. Due to channel porosity, the asymmetrical slip conditions are imposed on both walls. The coupled dimensionless partial differential equations are reduced to a system of second-order boundary-value problems based on some flow assumptions and solved by Adomian decomposition method (ADM). Variations in velocity and temperature profiles are presented and discussed in detail. The result of the analysis revealed that increasing Hartmann number decreases the flow velocity while the slip parameters enhance the flow.

1. Introduction

A large number of scientists have shown interest in oscillatory fluid flow due to its applications in cooling systems, monitoring of cardiovascular problems, movements of spermatozoa and lots more. Given these numerous applications, Wang [1] introduced an expression to tackle the problem associated with oscillatory flows in the steady-periodic regimes. Since many of the fluids with industrial applications are actually reactive in nature and undergo varying degree of exothermic or endothermic chemical interactions, Jha and Ajibade [2] examined the influence of a heat source/sink on the convective oscillatory flow that is controlled by suction and injection. In a related study, Adesanya [3] investigated the unsteady micro-channel flow induced by natural convection in a leaking channel taking slip and temperature jump into consideration. Other relevant studies on convective flow problems can be found in [4]-[5].

The above studies neglect the influence of magnetic field and Joulean heating on the convective suction/injection controlled fluid flow. In countless real-life situations, an external magnetic field is important in various fluid flows as a control strategy, for example, the concept is used in controlling hot moving steel in metallurgical engineering. It is also applied in the agglomeration of ferrofluid and other polar fluid particles even in targeted drug delivery in medicine. As a result, several researchers have worked on diverse applications of magnetohydrodynamics (MHD). For instance, Adesanya et al [6] analysed the influence of external magnetic field imposed across the vertical channel with time-periodic conditions. Abel and Mahesha [7] reported the hydromagnetic flow of a radiative fluid with variable thermal conductivity. Ibrahim and Shanker [8] studied of transient magnetohydrodynamics flow over a stretching sheet. Bég et al. [9] examined the magnetohydrodynamic flow in a rotating channel filled with porous materials. Other relevant studies on hydromagnetic convective heat transfer can be found in [10-23].

From the application viewpoint, a sounder assumption for flows over a porous channel is that of the slip since the velocity of the fluid can never match that of the solid boundaries. Therefore, in this paper, the asymmetrical Navier slip conditions will be used as opposed to the no-slip conditions imposed in [2]. Specifically, the main interest of this paper is to generalize the study reported by Jha and Ajibade [2] to the case in which fluid particles are electrically conducting and the slip effect at the leaky boundaries. The introduction of the Navier slip conditions and the dissipations due to viscous heating and magnetic field make the mathematical model more robust and enhance the usability in several real-life applications connected with flows through permeable walls. Under these assumptions, it is not plausible to get the exact solutions due to nonlinearities associated with the model, therefore, an approximate solution of the problem would be obtained. To validate the symbolic solutions, the out-coming results will be compared with existing ones in literature for validation. This semi-analytical approach has been used to obtain approximate solutions to different nonlinear problems in [24-33]. The choice of this method is because of its rapid convergence, avoidance of linearization or discretization and does not require the use of any simplifying assumptions.

In the next section, the mathematical analysis of the problem is presented. Section three dealt with the Adomian decomposition method of solution. In section four, graphical and numerical results presented and analysed while concluding notes are given in section five.

2. Mathematical Analysis

Consider the transient flow of a hydromagnetic heat-generating fluid in a vertical porous channel. Buoyancy is induced due to temperature changes in the fluid density and the periodic heating at the porous channels which were taken vertically to the x-axis at $y = \pm h$. A transverse magnetic field of strength B_0 is applied parallel to the x-axis as shown in Figure 1. We further assumed that heat generation within the channel is a linear function of temperature.

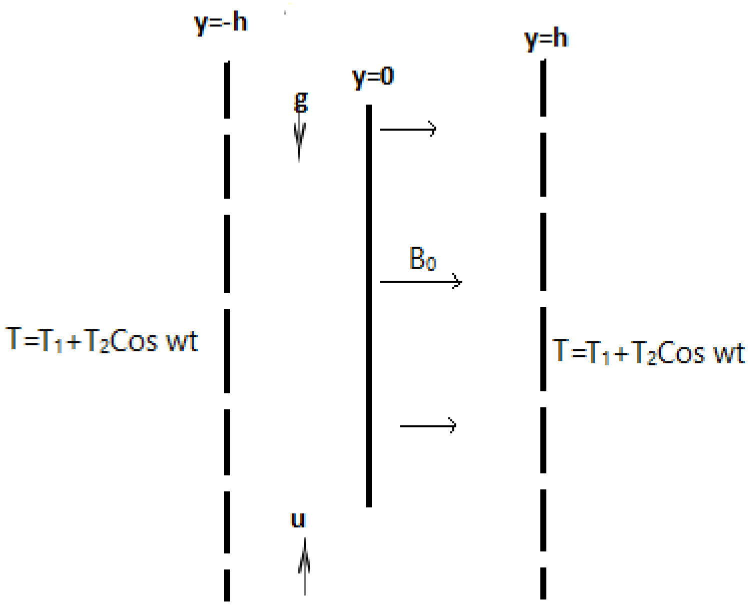

Figure 1: Problem geometry

Neglecting the induced magnetic field, the balanced equations for the fully thermally developed flow are [1]:

$$\left.\begin{aligned} &\frac{\partial u}{\partial t} - V_0\frac{\partial u}{\partial y} = \nu\frac{\partial^2 u}{\partial y^2} + g\beta(T-T_0) - \frac{\sigma B_0^{\,2}}{\rho}u, \\ &\frac{\partial T}{\partial t} - V_0\frac{\partial T}{\partial y} = \frac{k}{\rho C_P}\frac{\partial^2 T}{\partial y^2} - \frac{Q_0(T-T_0)}{\rho C_P} + \frac{\nu}{C_p}\left(\frac{\partial u}{\partial y}\right)^2 + \frac{\sigma B_0^{\,2}}{\rho C_P}u^2 \end{aligned}\right\} \tag{1}$$

Subject to slip and thermal conditions:

$$T = T_1 + T_2 Cos\left(\omega t\right)\Big|_{y=\pm h},\ \mathrm{u}\left(-h\right) = \gamma_1 \frac{du}{dy}\bigg|_{y=-h},\mathrm{u}\left(h\right) = -\gamma_2 \frac{du}{dy}\bigg|_{y=h} \tag{2}$$

Additional terms in (1) represent the imposed magnetic field, Ohmic and viscous heating effects. Following [1-6], the following expressions are introduced for separation of variables:

$$\left.\begin{aligned} u\left(t,y\right) &= \frac{g\beta h^2}{\nu}\left(\left(T_1 - T_0\right)A(\eta) + T_2 B(\eta)e^{iwt}\right), \\ T\left(t,y\right) &= T_0 + \left(T_1 - T_0\right)F(\eta) + T_2 G(\eta)e^{i\omega t}. \end{aligned}\right\} \tag{3}$$

using the following dimensionless variables and quantities

$$\begin{aligned} &\eta = \frac{y}{h}, \lambda = \frac{\left(g\beta h^2\right)^2 (T_1 - T_0)}{C_p \nu^2}, St = \frac{h^2\omega}{\nu}, \mathrm{Pr} = \frac{\mu C_p}{k}, \\ &Ha^2 = \frac{\sigma B_0^{\,2} h^2}{\mu}, s = \frac{hV_0}{\nu},\ \delta = \frac{Q_0 h^2}{k}, \phi_1 = \frac{\gamma_1}{h}, \phi_2 = \frac{\gamma_2}{h} \end{aligned} \tag{4}$$

Substituting equations (2) - (4) in equation (1) leads to the following coupled boundary-valued problems:

$$\left.\begin{aligned} &A''\left(\eta\right) + sA'\left(\eta\right) - Ha^2 A\left(\eta\right) = -F(\eta); \qquad A\left(-1\right) = \phi_1 A'\left(-1\right), A\left(1\right) = -\phi_2 A'\left(1\right) \\ &B''\left(\eta\right) + sB'\left(\eta\right) - \left(Ha^2 + iSt\right)B\left(\eta\right) = -G(\eta); \qquad B\left(-1\right) = \phi_1 B'\left(-1\right),\ B\left(1\right) = -\phi_2 B'\left(1\right) \\ &F''\left(\eta\right) + s\,\mathrm{Pr}\,F'\left(\eta\right) - \delta\,\mathrm{Pr}\,F\left(\eta\right) = -\mathrm{Pr}\,\lambda\left(A'^2(\eta) + Ha^2 A^2(\eta)\right); \quad F\left(\pm 1\right) = 1 \\ &G''\left(\eta\right) + s\,\mathrm{Pr}\,G'\left(\eta\right) - \left(\delta + iSt\right)\mathrm{Pr}\,G\left(\eta\right) = -2\,\mathrm{Pr}\,\lambda\left(A'(\eta)B'(\eta) + Ha^2 A(\eta)B(\eta)\right); \ G\left(\pm 1\right) = 1. \end{aligned}\right\} \tag{5}$$

In (5), the primes represent the derivative with respect to η. Kindly note that higher powers of $e^{i\omega t}$ have been neglected. It is obvious that the present result reduces to that obtained in [2] in the asymptotic case when $\left(\phi_1, \phi_2, \lambda, Ha^2\right) \to 0$, this condition would be used in the following section to establish the accuracy of our computation.

3. Adomian Method of Solution

The first step to be taken here in solving the system of equations (5) is to convert the boundary-value problem (5) to its equivalent Volterra integral equations form. i.e.

$$\left.\begin{aligned} &A\left(\eta\right) = a_0 + \int_{-1}^{\eta} a_1 dY + \int_{-1}^{\eta}\int_{-1}^{\eta}\left(Ha^2 A\left(Y\right) - s\frac{dA}{dY} - F\left(Y\right)\right)dYdY, \\ &B\left(\eta\right) = b_0 + \int_{-1}^{\eta} b_1 dY + \int_{-1}^{\eta}\int_{-1}^{\eta}\left(\left(iSt + Ha^2\right)B\left(Y\right) - s\frac{dB}{dY} - G\left(Y\right)\right)dYdY, \\ &F\left(\eta\right) = 1 + \int_{-1}^{\eta} f_0 dY + \int_{-1}^{\eta}\int_{-1}^{\eta}\left(\delta\,\mathrm{Pr}\,F(Y) - s\,\mathrm{Pr}\frac{dF}{dY} - \mathrm{Pr}\,\lambda\left(A'^2(Y) + Ha^2 A^2(Y)\right)\right)dYdY, \\ &G\left(\eta\right) = 1 + \int_{-1}^{\eta} g_0 dY + \int_{-1}^{\eta}\int_{-1}^{\eta}\left(\left(\delta + iSt\right)\mathrm{Pr}\,G\left(Y\right) - s\,\mathrm{Pr}\frac{dG}{dY} - 2\,\mathrm{Pr}\,\lambda\left(A'(Y)B'(Y) + Ha^2 A(Y)B(Y)\right)\right)dYdY. \end{aligned}\right\} \tag{6}$$

The standard Adomian decomposition method allows the following infinite series solutions:

$$A(\eta) = \sum_{n=0}^{\infty} A_n(\eta),\quad B(\eta) = \sum_{n=0}^{\infty} B_n(\eta),\quad F(\eta) = \sum_{n=0}^{\infty} F_n(\eta),\quad G(\eta) = \sum_{n=0}^{\infty} G_n(\eta). \tag{7}$$

Using (7) in (6) leads to

$$\left.\begin{aligned}
&\sum_{n=0}^{\infty} A_n(\eta) = a_0 + \int_{-1}^{\eta} a_1 dY + \int_{-1}^{\eta}\int_{-1}^{\eta}\left[Ha^2 \sum_{n=0}^{\infty} A_n(Y) - s\frac{d}{dY}\left(\sum_{n=0}^{\infty} A_n(Y)\right) - \sum_{n=0}^{\infty} F_n(Y)\right] dYdY,\\
&\sum_{n=0}^{\infty} B_n(\eta) = b_0 + \int_{-1}^{\eta} b_1 dY + \int_{-1}^{\eta}\int_{-1}^{\eta}\left[\left(iSt + Ha^2\right)\sum_{n=0}^{\infty} B_n(Y) - s\frac{d}{dY}\left(\sum_{n=0}^{\infty} B_n(Y)\right) - \sum_{n=0}^{\infty} G_n(Y)\right] dYdY,\\
&\sum_{n=0}^{\infty} F_n(\eta) = 1 + \int_{-1}^{\eta} f_0 dY + \int_{-1}^{\eta}\int_{-1}^{\eta} \delta \Pr \sum_{n=0}^{\infty} F_n(Y) - s\Pr\frac{d}{dY}\left(\sum_{n=0}^{\infty} F_n(Y)\right) dYdY,\\
&\qquad - \lambda \Pr \int_{-1}^{\eta}\int_{-1}^{\eta}\left(Ha^2\left(\sum_{n=0}^{\infty} A_n(Y)\right)^2 + \left(\frac{d}{dY}\sum_{n=0}^{\infty} A_n(Y)\right)^2\right) dYdY,\\
&\sum_{n=0}^{\infty} G_n(\eta) = 1 + \int_{-1}^{\eta} g_0 dY + \int_{-1}^{\eta}\int_{-1}^{\eta} (\delta + iSt)\Pr \sum_{n=0}^{\infty} G_n(Y) - s\Pr\frac{d}{dY}\left(\sum_{n=0}^{\infty} G_n(Y)\right) dYdY.\\
&\qquad - 2\lambda \Pr \int_{-1}^{\eta}\int_{-1}^{\eta}\left(\left(\frac{d}{dY}\sum_{n=0}^{\infty} A_n(Y)\right)\left(\frac{d}{dY}\sum_{n=0}^{\infty} B_n(Y)\right) + Ha^2\left(\sum_{n=0}^{\infty} A_n(Y)\right)\left(\sum_{n=0}^{\infty} B_n(Y)\right)\right) dYdY.
\end{aligned}\right\} \tag{8}$$

Similarly, the following nonlinear terms are identified in (8) above as:

$$\begin{aligned}
M_n &= Ha^2\left(\sum_{n=0}^{\infty} A_n(Y)\right)^2 + \left(\frac{d}{dY}\sum_{n=0}^{\infty} A_n(Y)\right)^2,\\
S_n &= \left(\frac{d}{dY}\sum_{n=0}^{\infty} A_n(Y)\right)\left(\frac{d}{dY}\sum_{n=0}^{\infty} B_n(Y)\right) + Ha^2\left(\sum_{n=0}^{\infty} A_n(Y)\right)\left(\sum_{n=0}^{\infty} B_n(Y)\right).
\end{aligned} \tag{9}$$

by Taylor's expansion (9) can be decomposed into Adomian polynomials

$$\left.\begin{aligned}
M_0 &= A_0^{'}(Y)^2 + Ha^2 A_0(Y)^2,\\
M_1 &= 2A_0^{'}(Y)A_1^{'}(Y) + 2Ha^2 A_0(Y)A_1(Y)\\
&....
\end{aligned}\right\} \tag{10}$$

and

$$\left.\begin{aligned}
S_0 &= Ha^2 A_0(Y)B_0(Y) + A_0^{'}(Y)B_1^{'}(Y),\\
S_1 &= Ha^2\left(A_0(Y)B_1(Y) + A_1(Y)B_0(Y)\right) + A_0^{'}(Y)B_1^{'}(Y) + A_1^{'}(Y)B_0^{'}(Y)\\
&....
\end{aligned}\right\} \tag{11}$$

by successive approximation, we then have the following recursive relations

$$\left.\begin{aligned}
&A_0(\eta) = a_0 + \int_{-1}^{\eta} a_1 dY,\ B_0(\eta) = b_0 + \int_{-1}^{\eta} b_1 dY\\
&F_0(\eta) = 1 + \int_{-1}^{\eta} f_0 dY,\ G_0(\eta) = 1 + \int_{-1}^{\eta} g_0 dY
\end{aligned}\right\} \tag{12}$$

with

$$\left.\begin{aligned}
A_{n+1}(\eta) &= \int_{-1}^{\eta}\int_{-1}^{\eta}\left(Ha^2 A_n(Y) - s\frac{dA_n}{dY} - F_n(Y)\right)dYdY,\\
B_{n+1}(\eta) &= \int_{-1}^{\eta}\int_{-1}^{\eta}\left(\left(iSt + Ha^2\right)B_n(Y) - s\frac{dB_n}{dY} - G_n(Y)\right)dYdY,\\
F_{n+1}(\eta) &= \int_{-1}^{\eta}\int_{-1}^{\eta}\left(\delta \Pr F_n(Y) - s\Pr\frac{dF_n}{dY} - \Pr\lambda M_n\right)dYdY,\\
G_{n+1}(\eta) &= \int_{-1}^{\eta}\int_{-1}^{\eta}\left(\left(\delta + iSt\right)\Pr G_n(Y) - s\Pr\frac{dG_n}{dY} - 2\Pr\lambda S_n\right)dYdY.
\end{aligned}\right\} \tag{13}$$

Few terms of (13) are required to obtain the partial sums

$$A(\eta) = \sum_{n=0}^{m} A_n(\eta),\ B(\eta) = \sum_{n=0}^{m} B_n(\eta), F(\eta) = \sum_{n=0}^{m} F_n(\eta),\ \ G(\eta) = \sum_{n=0}^{m} G_n(\eta) \tag{14}$$

since (14) are convergent and twice differentiable. Using the remaining boundary conditions in (5), expressions for the unknown parameters a_0, b_0, f_0, g_0 are obtained. Based on the approximate solution (14), the skin friction and the rate of heat transfer within the flow channel are then computed respectively as follows:

$$S_f = \frac{dB}{dy},\ Nu = -\frac{dG}{dy}. \tag{15}$$

4. Results and Discussion

In this section, equations (10)-(15) are carefully coded on a symbolic package MATHEMATICA 8.0 for easy iteration of the numerical integration. The process generated a huge symbolic solution that is too large to be included in this write-up, hence, only the graphical results are presented (see Figures 2-5). As mentioned previously, the result obtained in [2] has been benchmarked for validation purpose and is therefore presented in Tables 1-2. An excellent agreement is observed and this confirms the reliability of ADM in the handling of coupled boundary value problems.

Table 1: Convergence of solutions for velocity field when $m = 10,\ Ha = 0 = \phi_{1,2}$

y	$A(\eta)_{Exact}$ [2]	$A(\eta)_{ADM}$	Absolute Error	$B(\eta)_{Exact}$ [2]	$B(\eta)_{ADM}$	Absolute Error
1	0	0	0	0	0	8.88178E-16
-0.75	0. 191594	0. 191594	3.26719E-07	0.141466	0.141469	3.51418-06
-0.5	0.29587	0.29587	5.99328E-07	0.213966	0.213973	6.4098E-06
-0.25	0.337939	0.337939	8.44888E-07	0.243139	0.243148	8.93325E-06
0	0.33390	0.333899	1.08159E-06	0.24283	0.242842	1.12249E-05
0.25	0.293727	0.293726	1.31072E-06	0.218953	0.218966	1.33138E-05
0.5	0.223180	0.223178	1.4695E-06	0.172309	0.172324	1.48667E-05
0.75	0.125056	0.125055	1.28901E-06	0.100621	0.100634	1.36999E-05
1	0	0	0	0	0	2.22405E-16

Table 2: Convergence of solutions for temperature field when $m = 10,\ Ha = 0 = \phi_{1,2}$

y	$F(\eta)_{Exact}$ [2]	$F(\eta)_{ADM}$	Absolute Error	$G(\eta)_{Exact}$ [2]	$G(\eta)_{ADM}$	Absolute Error
1	1	1	2.22045E-16	1	1	4.44089E-16
-0.75	0.808406	0.808406	3.26719E-07	0.77398	0.77398	2.1644E-07
-0.5	0.704130	0.704130	5.99328E-07	0.648087	0.648086	3.61845E-07
-0.25	0.662061	0.662061	8.44888E-07	0.596908	0.596908	4.30082E-07
0	0.666100	0.666101	1.08159E-06	0.602555	0.602555	4.15985E-07
0.25	0.706273	0.706274	1.31072E-06	0.652739	0.652739	3.27111E-07
0.5	0.776820	0.776822	1.46950E-06	0.739168	0.739168	2.27333E-07
0.75	0.874944	0.874946	1.28901E-06	0.856242	0.856242	2.40399E-07
1	1	1	1.11022E-16	1	1	4.44089E-16

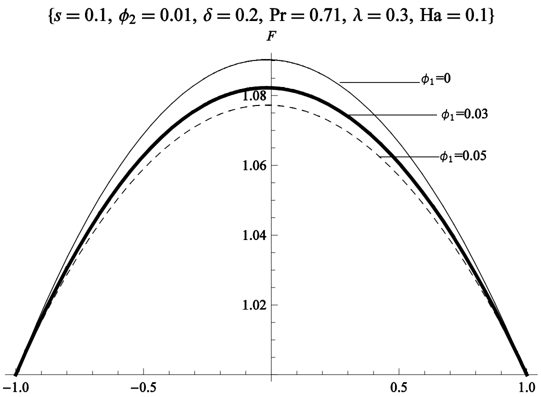

2a) Effects of suction Navier slip

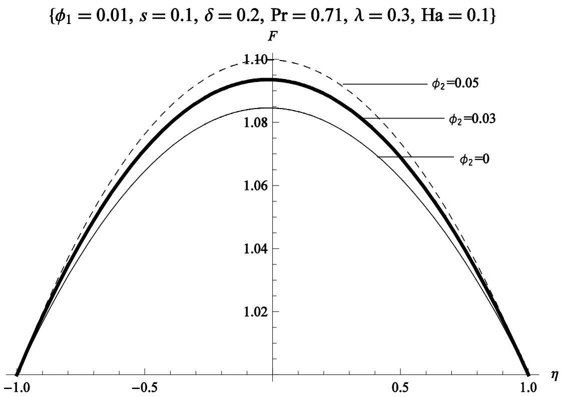

2b) Effects of injection Navier slip

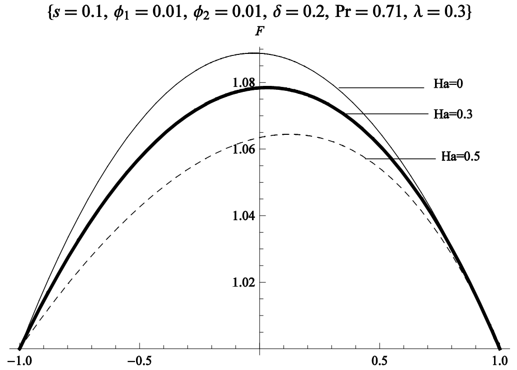

2c) Effects of Hartmann number

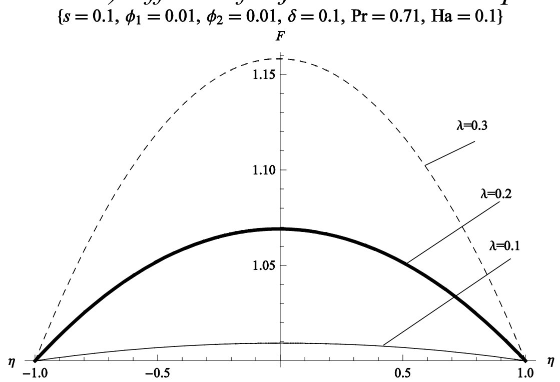

2d) Effects of viscous heating parameter

Figure 2: Effects of parameters on steady temperature regimes

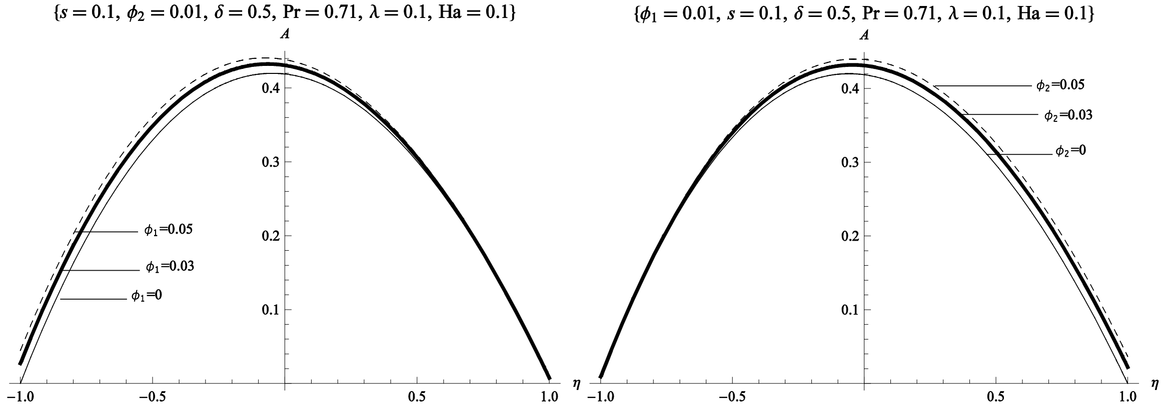

3a) Effects of suction Navier slip *3b) Effects of injection Navier slip*

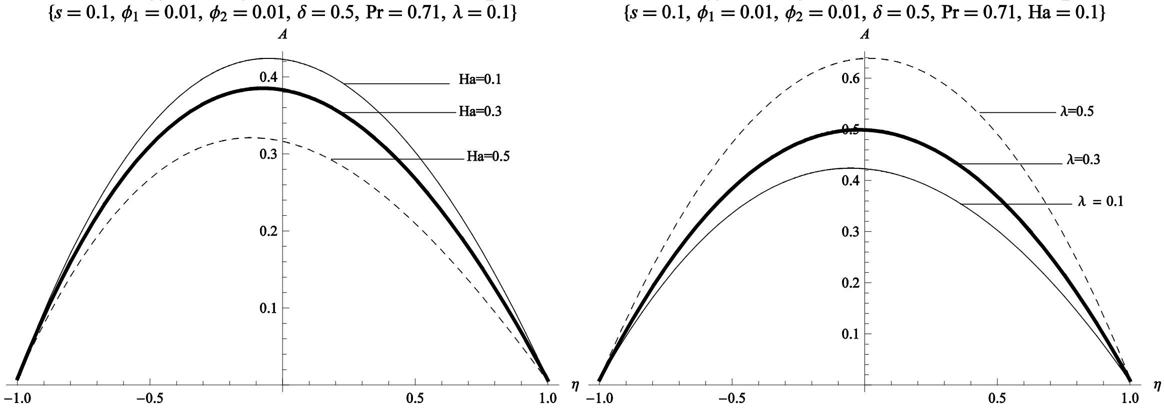

3c) Effects of Hartmann number *3d) Effects of viscous heating parameter*

Figure 3: Effects of parameters on steady flow regimes

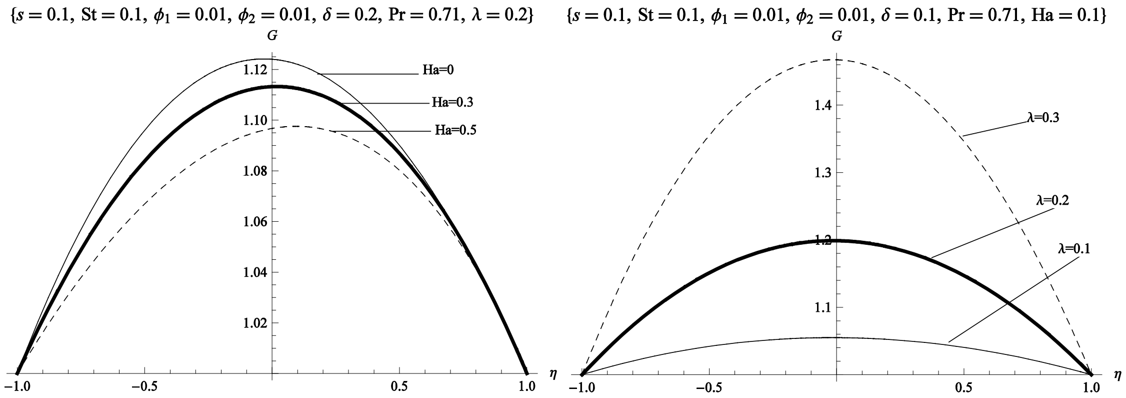

4a) Effects of Hartmann number *4b) Effects of viscous heating parameter*

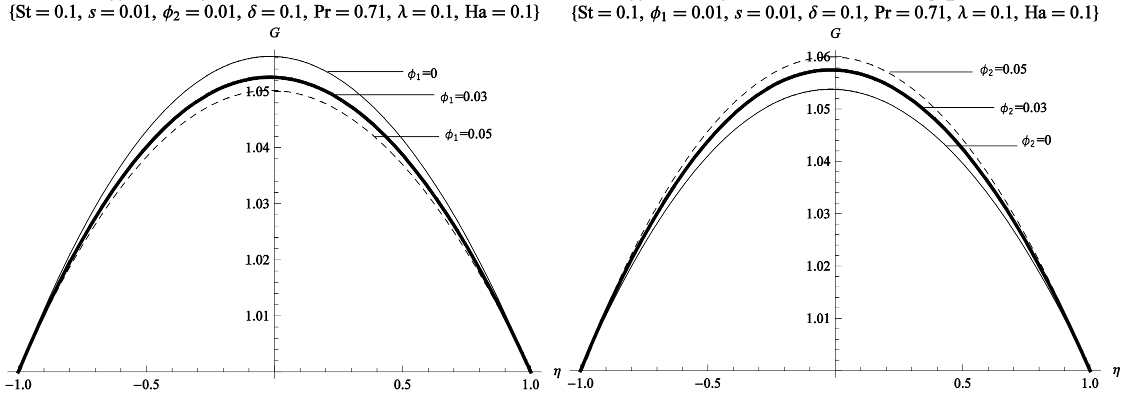

4c) Effects of injection Navier slip *4d) Effects of suction Navier slip*

Figure 4: Effects of parameters on periodic temperature regimes

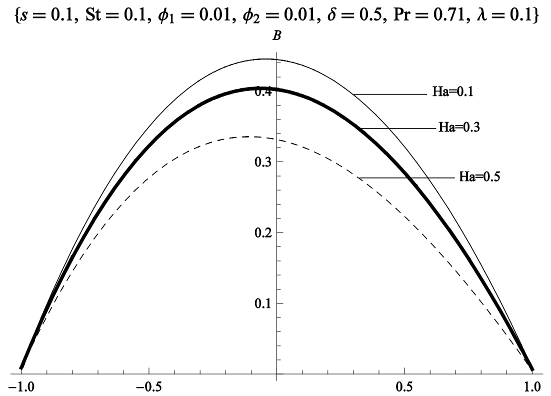

5a) Effects of Hartmann number

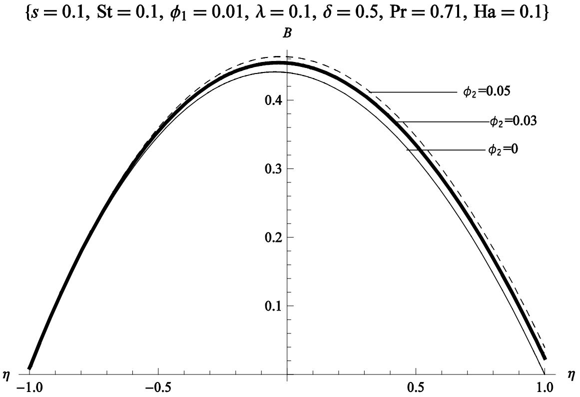

5b) Effects of suction Navier slip

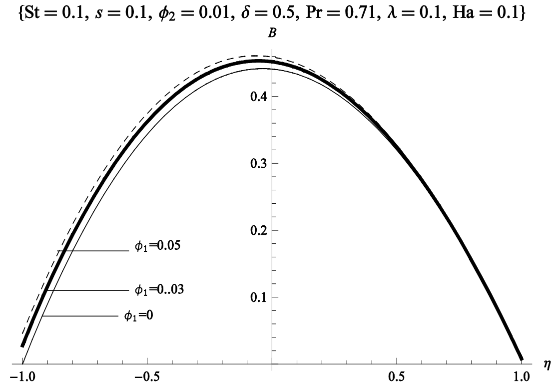

5c) Effects of injection Navier slip

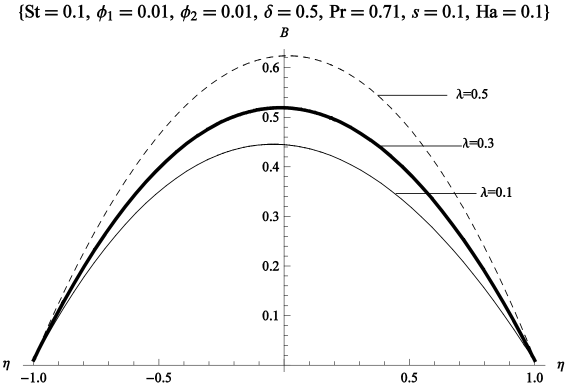

5d) Effects of viscous heating parameter

Figure 5: Effects of parameters on periodic velocity regimes

Figure 2 presents the effect of variation of the parameter on the temperature distribution in the steady flow regime. Figure 2a represents the effect of suction Navier slip on the fluid temperature. As observed from the plot, an increase in the suction Navier slip parameter is seen to decrease the temperature profile. This is physically corrected since heat is sucked away from the leaky channel. Similarly in Figure 2b, one observed that as the injection slip parameter increases, there is a corresponding increase in the slip length as fluid is being injected into the channel, as a result, the temperature increases accordingly. In Figure 2c, the effect of magnetic field on the temperature field in the steady regime is presented. As observed from the plot, an increase in the magnetic field intensity i.e. Hartmann number placed across the flow channel is seen to decrease the fluid temperature due to the reduced flow induced by the resistive effect of Lorentz forces. In Figure 2d, the effect of viscous heating on the fluid temperature is shown. As the viscous heating parameter increases, the fluid temperature is observed to be on the increase due to the increased thermal expansion of the fluid particles.

In Figure 3a, b the effect of asymmetrical slip parameter on the fluid flow is presented. From the results, increasing the suction slip parameter enhances the flow velocity at the suction wall as the slip length increases similar behaviour is experienced at the injection wall of the porous channel. Moreover, in Figure 3c, the effect of Ohmic heating of the electrically conducting fluid is presented. It is important to note here that as the magnetic field intensity parameter (Hartmann number) increases there is a corresponding decrease in the dynamic viscosity of the fluid. This is true since an increase in Hartmann number of the electrically conducting fluid implies that the Lorentz force $F = j \times B_0$ generated due to the interaction between the magnetic induction B_0 and the electric current density j that is induced by Faraday's law in liquid metals increases. This ultimately agglomerates the ferrofluid particles thus decreasing the fluid flow velocity. However, in Figure 3d, the effect of viscous dissipation on the fluid flow is presented. Being heat source, the heat dissipated within the flow channel has melting effect on the fluid hence an increased fluid flow. It is interesting to note that the periodic regimes presented in Figures 4-5 above follow the same trend with the steady flows except that the magnitude is much lower due to increasing frequency of heating.

5. Concluding Remarks

This paper studied the MHD free convective slip flow variable heat loss subjected to time-periodic boundary conditions. Approximate solutions of the coupled problem are obtained via ADM, validated and are shown to be convergent. Future analysis can include using Homotopy analysis method [35]-[36] for the coupled convective problem.
Summarily, the main contributions to knowledge are as follows:

i. increasing values of *Ha* decreases the fluid flow velocity due to retarding action of Lorentz forces.
ii. asymmetrical Navier slip enhances the fluid velocity at both injection and suction walls.
iii. viscous heating elevates the temperature distribution of the suction/injection controlled flow.

Nomenclature

$A(\eta)$ & $B(\eta)$	- steady and periodic velocity components respectively
$F(\eta)$ & $G(\eta)$	- steady and periodic temperature regimes
g	- gravitational acceleration
h	- channel half width
Cp-	- specific heat capacity at constant pressure
δ	- coefficient of linear internal heat generation/absorption
Pr	- Prandtl number
St	- Strouhal number that describes the heating frequency
t-	- dimensionless time
(T_0, T_1, T_2)	- referenced fluid temperatures
T-	- fluid temperature
u-	- fluid velocity,
x', y'	-cartesian co-ordinates
β	- coefficient of thermal expansion
μ	- dynamic viscosity
υ	- kinematic viscosity
ω-	- frequency of periodic heating
σ -	- electrical conductivity
B_0 -	- magnetic field intensity
ρ -	- fluid density
Ha^2-	- Hartmann number
λ	- viscous heating parameter
$\gamma_{1,2}$	- slip length at porous walls
(ϕ_1, ϕ_2)	- suction and injection Navier slip parameters respectively.

References

[1] C. Y. Wang Free convection between vertical plates with periodic heat input. ASME J Heat Trans 110 (1988) 508–11.

[2] B K. Jha, and A. O Ajibade, Free convective flow of heat generating/absorbing fluid between vertical porous plates with periodic heat input, International Communications in Heat and Mass Transfer, 36 (2009) 624–631

[3] S. O. Adesanya, Free convective flow of heat generating fluid through a porous vertical channel with velocity slip and temperature jump, Ain Shams Eng J (2015), vol. 6(3) pp 1045-1052

[4] B K. Jha, and A. O Ajibade, Free convective flow between vertical porous plates with periodic heat input, ZAMM· Z.A.M.M., (2010) 1 – 9, DOI10.1002/zamm.200900268

[5] B K. Jha, and A. O Ajibade, Effect of viscous dissipation on Natural convection flow between vertical parallel plates with time-periodic boundary conditions, Commun. Nonlinear Sci Numerical Simulat 17 (2012) 1576 -1587

[6] S.O. Adesanya, E. O. Oluwadare, J.A. Falade, O.D. Makinde, Hydromagnetic natural convection flow between vertical parallel plates with time-periodic boundary conditions, Journal of Magnetism and Magnetic Materials, http://dx.doi.org/10.1016/j.jmmm.2015.07.096

[7] M. Subhas Abel and N. Mahesha, Heat transfer in MHD viscoelastic fluid flow over a stretching sheet with variable thermal conductivity, non-uniform heat source and radiation, Applied Mathematical Modelling 32 (2008) 1965–1983

[8] W. Ibrahim and B. Shanker, Unsteady MHD boundary-layer flow and heat transfer due to stretching sheet in the presence of heat source or sink, Computers & Fluids 70 (2012) 21–28

[9] O. Anwar Bég, Lik Sim, J. Zueco, R. Bhargava, Numerical study of magnetohydrodynamic viscous plasma flow in rotating porous media with Hall currents and inclined magnetic field influence, Commun Nonlinear Sci Numer Simulat 15 (2010) 345–359

[10] O. Anwar Bég, M.J. Uddin, M.M. Rashidi, N. Kavyani, Double-diffusive radiative magnetic mixed convective slip flow with Biot and Richardson number effects, J. Eng. Thermophy. 23 (2014) 79–97.

[11] T. Hayat, A. Shafiq, A. Alsaedi, M. Awais, MHD axisymmetric flow of third grade fluid between stretching sheets with heat transfer, Computers & Fluids Volume 86, 5 2013, Pages 103–108

[12] T. Hayat, S.A. Shehzad, S. Asghar, MHD flow, thixotropic fluid thermal radiation, variable thermal conductivity and thermal radiation, Walailak J. Sci. Technol. 10 (1) (2013) 29–42.

[13] T. Hayat, R. Ellahi, F.M. Mahomed, The analytical solution for magnetohydrodynamic flow of a of third order fluid in porous medium, Zeitschrift Fur Naturforschung A 64 (a) (2009 531–539.

[14] R. Ellahi, A. Riaz, Analytical solution for MHD flow in a third grade fluid with variable viscosity, Math. Comput. Model. 5 (2010) 1783–1793.

[15] T. Hayat, A.H. Kara, Couette flow of a third-grade fluid with variable magnetic field, Math. Comput. Model. 43 (2006) 132 137.

[16] A. Shafiq, M. Nawaz, T. Hayat, A. Alsaedi Magnetohydrodynamic axisymmetric flow of a third-grade fluid between two porous disks, Brazilian J. Chem. Eng. 3 (2013) 599–609.

[17] Sheikholeslami, M.; Ganji, D. D.; Rashidi, M. M., Magnetic field effect on unsteady nanofluid flow and heat transfer using Buongiorno model, Journal of Magnetism and Magnetic Materials ,16(2016)164-173

[18] M. Sheikholeslami, M.M. Rashidi, T. Hayat, D.D. Ganji, Free convection of magnetic nanofluid considering MFD viscosity effect, Journal of Molecular Liquids 218 (2016) 393-399

[19] M Sheikholeslami, Davood Domiri Ganji, Entropy generation of nanofluid in presence of magnetic field using Lattice Boltzmann Method, Physica A 417 (2015) 273-286

[20] M. Sheikholeslami, ; Domiri Ganji, Davood; Younus Javed, M.; Ellahi, R., Effect of thermal radiation on magnetohydrodynamics nanofluid flow and heat transfer by means of two phase model, Journal of Magnetism and Magnetic Materials 374 (2015) 36-43

[21] M. Sheikholeslami, Houman B. Rokni, Nanofluid two phase model analysis in existence of induced magnetic field, International Journal of Heat and Mass Transfer 107 (2017) 288-299,

[22] T. Hayat, M. Qasim, S. Mesloub, MHD flow And Heat Transfer Over Permeable Stretching Sheet With Slip Conditions, International Journal For Numerical Methods In Fluids, 66, 963–975, 2011

[23] M. Sheikholeslami, M. Gorji-Bandpy, D.D. Ganji, P. Rana, Soheil Soleimani, Magnetohydrodynamic free convection of Al_2O_3–water nanofluid considering Thermophoresis and Brownian motion effects, Computers & Flu ids, 94, 2014, Pages 147–160

[24] G. Adomian and R. Rach, Transformation of series, Applied Mathematics Letters, vol. 4, no. 4, pp. 69–71, 1991.

[25] R. Rach, G. Adomian, and R. E. Meyers, A modified decomposition, Computers and Mathematics with Applications, vol. 23, no. 1, pp. 17–23, 1992.

[26] G. Adomian, Modification of the decomposition approach to the heat equation, Journal of Mathematical Analysis and Applications, vol. 124, no. 1, pp. 290–291, 1987.

[27] G. Adomian, A new approach to the heat equation—an application of the decomposition method, Journal of Mathematical Analysis and Applications, vol. 113, no. 1, pp. 202–209, 1986.

[28] R. Rach, A convenient computational form for the Adomian polynomials, Journal of Mathematical Analysis and Applications, vol. 102, no. 2, pp. 415–419, 1984.

[29] S. O. Adesanya, Linear Stability Analysis of a plane-Poiseuille hydromagnetic Flow Using Adomian Decomposition Method, U.P.B. Sci. Bull., Series A, 75, 2013, 99-106.

[30] S. O. Adesanya and O. D. Makinde, Thermodynamic analysis for a third-grade fluid through a vertical channel with internal heat generation, Journal of Hydrodynamics, 2015,27(2):264-272

[31] S. O. Adesanya and O. D. Makinde, Entropy generation in couple stress fluid flow through porous channel with fluid slippage, Int. J. Exergy, Vol. 15, No. 3, 2014

[32] S. O. Adesanya and O. D. Makinde, Effects of couple stresses on entropy generation rate in a porous channel with convective heating, Comp. Appl. Math. (2015) 34:293–307

[33] M. Sheikholeslami, D.D. Ganji, H.R. Ashorynejad, Investigation of squeezing unsteady nanofluid flow using ADM, Powder Technology 239 (2013) 259-265.pages 529-553

[35] Srinivas Jangili and O. Anwar Bég , Homotopy study of entropy generation in magnetized micropolar flow in a vertical parallel plate channel with buoyancy effect, Heat Transfer Research, DOI: 10.1615/HeatTransRes.2018018305 pages 529-553

[36] J. Srinivas, J.V. Ramana Murthy, Ali J Chamkha, (2016) "Analysis of entropy generation in an inclined channel flow containing two immiscible micropolar fluids using HAM", International Journal of Numerical Methods for Heat & Fluid Flow, Vol. 26 Issue: 3/4, pp.1027-1049,https://doi.org/10.1108/HFF-09-2015-0354